EPJ Web of Conferences **292**, 05001 (2024) https://doi.org/10.1051/epjconf/202429205001
NRM2023

Transport model comparisons for intermediate-energy heavy-ion collisions

Hermann Wolter[1,*]

[1]Faculty of Physics, Ludwig-Maximilians-University, D-80799, Munich, Germany

Abstract. Transport model comparisons under controlled conditions are performed in order to evaluate the robustness of their predictions in heavy-ion collisions (HICs). Including many of the currently used transport codes comparisons are done in periodic boxes and for typical HICs at intermediate energies in the hadronc regime. In this way we succeed to understand the different results between codes and evaluate different simulation strategies. Ways to arrive at an uncertainty quantification of transport model studies are discussed.

1 Introduction

An important issue in nuclear physics and astrophysics is the determination of the nuclear equation-of-state (EOS), i.e. the energy density of infinite nuclear matter as a function of the macroscopic observables density, temperature, and neutron-proton asymmetry. It connects the fields of nuclear structure and direct reactions, the main topics of this conference, with the nature of astrophysical objects and processes, like neutrons stars (NSs), NS mergers, and core-collapse supernovae. Since astrophysical objects have large asymmetries at densities up to several times the saturation density ρ_0, the asymmetry-dependence of the EOS, called the nuclear symmetry enery (SE), and, particularly, its density dependence, are of great importance.

In the laboratory the high-density behaviour of the EOS can be studied with heavy-ion collisions (HICs) in which short-lived states of high density can be produced. An extensive review of the status and the prospects of this field as a White Paper has very recently been published in Ref. [1]. Here, we are concerned with densities where a description in terms of hadrons, their excited states, and mesons is appropriate, which corresponds to bombarding energies up to several GeV/A, to the so-called intermediate energy domain. The density behaviour of the EOS is studied in nuclear structure and direct reactions at and below saturation density. On the other hand, increasingly accurate constraints on high-density n-rich matter in the range 2- 5 ρ_0 are obtained from observations of NS radii and masses, particularly in simultaneous constraints on these from gravitational wave and NS mergers. HICs give information on the EOS from low densities in Fermi-energy collisions to about 3-5 ρ_0 at intermediate energies [1, 2]. They can bridge the gap in density between nuclear structure information and astrophysical observations. Thus, the study and interpretation of HICs is of great importance in the larger picture of the search for the nuclear EOS.

However, HICs create states of high density for very short time spans of the order of 10^{-22} to 10^{-21} s, in which not all parts of the colliding system reach thermal equilibrium. Thus the

*e-mail: hermann.wolter@lmu.de

interpretation of HICs requires a non-equlibrium approach, which is usually approximated by semi-classical transport theories. Their equations are of high complexity, as discussed in more detail below, and cannot be solved analytically nor by direct numerical methods, like lattice methods, which are computationally very demanding and have only been done in low-dimensional toy models. The usual method are simulations of the equations, which involve strategic decisions, which are not fixed by the equations themselves. This then raises the question of the robustness of inferences from transport studies of HICs on the EOS.

A recent example is given in Ref. [3], where pion production was studied in Sn+Sn collisions at 270 MeV/A. Several transport codes were asked to predict pion production in this reaction using their best physics model without prior knowledge of the data. In particular, the ratio of the yield of negative to positive pions, $Y(\pi^-)/Y(\pi^+)$, is considered to be a good probe of the SE at densities above saturation, since it should reflect the n/p asymmetry of the matter, where the pions are produced, and is easier to measure than the n/p ratio. It was seen in Ref. [3] that the different codes differed considerable between each other and from the experimental values, revealed afterwards, such that a determination of the high-density SE was hardly possible.

From these and similar previous experiences the question arises on the model-dependence of transport analyses of HICs, referring to different implementations, i.e. different codes, of transport equations. A way to obtain information on this, is to compare results of simulations by different codes for the same colliding system, as was already done very early in the development of transport descriptions of HICs, e.g. in Ref. [4]. Such comparisons were put on a more systematic basis by the Transport Model Evaluation Project (TMEP), starting in 2009 (though this name was attached later), where comparisons were made under controlled conditions, i.e., making the physics input and certain simulation parameters as identical as possible, and by comparing the time evolution of the collisions, as well as the final observables. A detailed review of these comparisons and their results, as well as a description of the participating codes, was given recently in Ref. [5]. The comparison was first done for HICs in the intermediate energy range of 100 - 400 MeV/A, and difference in observables were found of about 15-30 %, depending on the incident energy. To obtain a better understanding of these differences , simulations were compared in a box with periodic boundary conditions, which approximates infinite matter, and for which analytical or exact numerical results are often available.

This conference report is a brief review of these efforts and of their results so far. It will be seen, that we do not achieve to make the results of the different codes completely convergent, but, on the other hand, can understand the differences in detail as due to different strategies and procedures of the simulations. In many cases we can recommend best procedures, but cannot, of course, enforce implementation in all codes. In the last section we will dicuss possible avenues how to quantify the uncertainty of transport model analyses of HIC as a whole.

2 Transport approaches

Transport equations are derived from a general non-equilibrium quantum formalism in the framework of the real-time Martin-Schwinger Greeen function formalism [6], and after a truncation of the Bogoliubov-Green-Kirkwood-Yvon (BBGKY) hierarchy are formulated in the Kadanoff-Baym equations for the generalized 1-body Green function [7]. With a semi-classical approximation and a quasi-particle approximation, which neglects the finte width of the spectral functions of all particles, one arrives at a transport equation of the Boltzmann-Vlasov type, which describes the temporal evolution of the 1-body phase-space distribution of a particle species a, $f_a(\vec{r}, \vec{p}; t)$, under the action of a mean field and a dissipation process,

due to the average action of 2-body collisions [8, 9]. In non-relativistic form one obtains the equation

$$\Big(\frac{\partial}{\partial t} + \vec{\nabla}_p\epsilon\cdot\vec{\nabla}_r - \vec{\nabla}_r\epsilon\cdot\vec{\nabla}_p\Big)f_a(\vec{r},\vec{p};t) = I_{\rm coll}[f_a(\vec{r},\vec{p};t)], \tag{1}$$

where $\epsilon[f]$ is the single-particle energy, non-relativistically given as $\epsilon = \vec{p}^{\,2}/2M + U(\rho) + M$, where the mean-field potential in general is momentum-dependent and is often derived from a density functional, and $I_{\rm coll}$ is the collision integral due to the two-body scattering $p + p_b \rightarrow p' + p'_b$,

$$\begin{aligned} I_{\rm coll}[f_a] \;=\; & \sum_b \frac{g_b}{(2\pi\hbar)^3}\int d^3p_b\, d\Omega'\, v_{ab}\,\frac{d\sigma_{ab}^{\rm med}}{d\Omega'} \\ & [(1-f_a)(1-f_b)f'_af'_b - f_af_b(1-f'_a)(1-f'_b)]\;\delta(p+p_b-p'+p'_b). \end{aligned} \tag{2}$$

The distribution functions in Eq.(2) are all taken at the same position $\vec{r}$ and time t, and the momenta $\vec{p}\,'$ and $\vec{p_b}'$ are determined by energy-momentum conservation and the scattering angle Ω'. The summation b in the simplest case is over neutrons and protons and g_b is the spin degeneracy, but it may be extended to include other particle species with evolution equations of their own phase-space densities of the type of Eq.(1). In the above, $d\sigma_{ab}^{\rm med}/d\Omega$ are the in-medium nucleon-nucleon elastic differential scattering cross sections, or, for the case of other particle species, the corresponding inelastic cross sections, and the v_{ab} are the relative velocities. In the collision term one can see gain and loss terms, and the Pauli blocking factors $(1-f)$, which are included to preserve the fermionic character of the system. Corresponding equations for relativistic kinematics as well as for covariant Relativistic-Mean-Field models exist and are used [10]. In this form the equations are known by several names, but most often referred to as Boltzmann-Uehling-Uhlenbeck (BUU) equations.

The integro-differential non-linear BUU equations are solved numerically by simulations. To this end, the distribution functions f_a are represented in terms of a sum of finite elements, called test particles (TP), as

$$f_a(\vec{r},\vec{p};t) = \frac{1}{g_aN_{TP}}\Big(\frac{2\pi}{\hbar}\Big)^3\sum_{i=1}^{N_aN_{\rm TP}} G(\vec{r}-\vec{R}_i(t))\,\tilde{G}(\vec{p}-\vec{P}_i(t)) \tag{3}$$

where N_a is the number of particles of type a, N_{TP} the number of TP per particle, $\vec{R}_i$ and $\vec{P}_i$ are the time-dependent coordinates and momenta of the TPs, and G and $\tilde{G}$ are the profile functions in coordinate and momentum space, respectively, e.g. δ functions or normalized Gaussians. When δ functions are adopted for the profile functions the left-hand of the BUU equation, the Vlasov part, results in Hamiltonian equations of motion for the TP propagation. For finite-size profile functions the lattice-Hamiltonian methods of Ref. [11] have to be used.

The collision term is commonly evaluated by performing stochastic TP collisions with a criterion to decide when two TP collide and a random choice of the final directions, and by evaluating the final state blocking factors [12]. In principle, in the limit $N_{TP} \rightarrow \infty$ one obtains an exact deterministic solution of the equations; in practice, with a finite number of TPs, numerical fluctuations are introduced and their magnitude is controlled by the number and shape of the TPs (and can be chosen to simulate physical instabilities). A theoretically better founded treatment of fluctuations in the BUU formalism is provided by adding a fluctuation term on the rhs of Eq.(1) in the Boltzmann-Langevin formalism [13], which is done approximately in some codes.

A second family of transport approaches has been developed, known as Quantum Molecular Dynamics (QMD) [14], in which the many-body state is assumed as a simple product wave

function of single-particle states, in some cases generalized to include anti-symmetrization in the Antisymmetrized Molecular Dynamics (AMD) approach [15]. Although this ansatz corresponds to a single-particle mean-field approach, the description in terms of localized wave packets (wp) introduces classical many-body correlations. The propagation of the wps is similar to BUU with $N_{TP} = 1$ and the collision term is treated by similar methods, however, for collisions of nucleons and not of TPs. The shape of the wps is usually assumed as a Gaussian with fixed width Δx in coordinate space and a δ-function in momentum space. Due to this representation of the phase space QMD simulations show large fluctuations, which are regulated by the width parameter of the wp, which is only roughly constrained by the range of the interaction and by the requirement of a reasonable representation of the surface thickness of the initial state. QMD acts as an event generator with much larger fluctuations than in BUU in each event, and the events are averaged over finally. From a more general point of view BUU and QMD models follow different philosopies of describing the fluctuations, which have to be present in a HIC, and which are important for the outcome. In BUU they are not present in the formulation of Eq.(1), but have to be introduced by a fluctuation term, while in QMD they are introduced classically in the ansatz of the wave function. Thus one cannot expect that the two approaches will give identical results. Which of these approaches is more successful in describing the physical system is a matter of current debate.

In the controlled TMEP comparisons, which will be reviewed in the next sections, we prescribe the physics model, i.e., the mean-field potential and the elastic (and, depending on the case, inelastic) cross sections. We use relatively simple models, e.g. constant elastic cross sections and a momentum-independent mean field, since the object is not a detailed description of data, but the evaluation of the convergence of the codes. We provide a common initialization, since previous studies showed an influence of different inital states. Otherwise the strategies of the simulations are left to the codes as in their normal use, and we try to analyze and understand the differences. The participating codes of BUU- and QMD-type are identified in the figures in the following sections by the names given by their authors. They cannot be discussed in detail here, but a list of their names with references and a detailed description of their properties is given in Ref. [5].

One should realize that HICs are open systems, such that the different aspects of a simulation interact and small effects can lead to large differences in the final observables. To disentangle such effects, box calculations with periodic boundary conditions are useful, since these can be considered as closed systems with fixed average density, energy densitiy and isospin asymmetry, and they necessarily reach an equilibrium corresponding to the properties of the respective code. Thus individual aspects of a simulation, such as the mean-field propagation or the Pauli blocking in the collision term, can be investigated and compared separately. Also, analytical or exact numerical results exist in many cases and serve as a baseline for the comparisons. In the following, we first discuss a selection of results of box calculations and then the results of a recent comparison of pion production in a HIC.

3 Box calculations

In a first example we study the mean-field evolution of the phase space distribution, given by the rhs of Eq.(1), also known as the Vlasov equation, in a box, see also Ref. [16] where many more details are given. One would think that this is rather unproblematic, but, in fact, we observe sizable differences in the simulations due to effects of the fluctuations. In this comparison we turn off the collision term and imprint on the box initially a sinusoidal oscillation in z-direction and compare the evolution in a mean field, which is assumed to have a non-linear component proportional to ρ^γ with $\gamma > 2$, which is often introduced to effectively include the action of many-body forces. By Fourier transforming the evolving density with

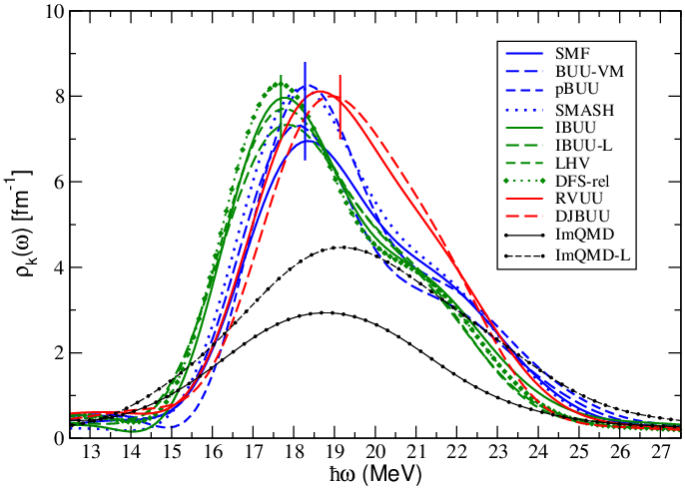

Figure 1. Response function $\rho_k(\omega)$, i.e., the Fourier transform with respect to space and time of the averaged density distribution in the box, from the different participating codes [16]. The results for the BUU codes are grouped according to their treatment of the dynamics (and are distinguished by the color of the lines): non-relativistic kinematics (blue), relativistic (green), covariant (red). The vertical lines indicate the analytical results from Fermi-liquid theory for the different code types, see text.

respect to space and time one obtains the response function or power spectrum. The results comparing many codes of BUU- and QMD-type with various tratments of relativity is shown in figure 1. One can see a broad peak around the imprinted mode with a broadening due to damping (by fluctuatons) and mode-mixing (by the non-linar term). BUU codes show a stronger, less damped, narrower response. The curves are color-coded with respect to the treatment of relativity (green - non-relativistic, blue - relativistic kinematics, and red - covariant formulation). In the small amplitude limit exact results can be obtained from Fermi-liquid theory for the zero-sound modes [16]. These results in the same color-coding are given by the short vertical lines, and one observes a good agreement for the BUU codes. QMD results are given by the black lines with dots (for one code, since in this case with common initial coditions and without collisions all QMD codes give the same result). The QMD response is broader, due to the stronger fluctuations. The peak position is influenced by an approximation used by many QMD codes of evaluating the non-linear force term, which is more critical for larger fluctuations. With more numerical effort this approximation can be avoided (in the IMQMD-L code, black dashed line with dots), which exhibits a stronger response and a shift of the peak position.

In another example of box analyses we study the Pauli blocking in the collision term in a cascade calculation with the mean field turned off [17]. The box is initialized at normal density and temperature T=5 MeV. The resulting collision rates after equilibration are shown in figure 2 for BUU (left) and QMD codes (right) with square symbols (disregard the star symbols here). Exact numerical results are a represented by the solid lines. If the Pauli blocking is turned off all codes agree well with each other and with the anylytical results (not shown, see [17]). The differences seen in figure 2 are thus due to the Pauli blocking of the final states in each 2-body collision, which exhibit fluctuations due to the numerical evaluation of the final state phase space occupation. Fluctuations make the blocking less effective and increase the collision rates. BUU codes with a finite number of TPs show moderate deviations

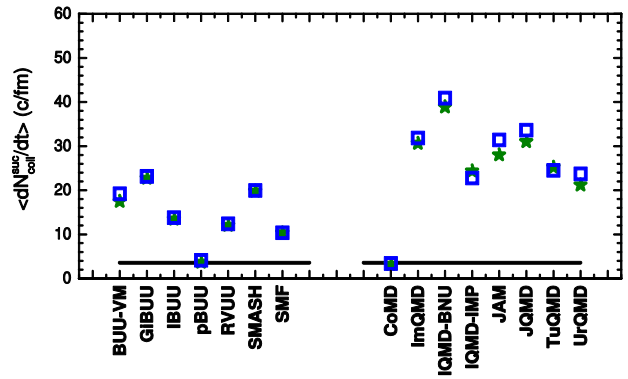

Figure 2. Collision rates from the different models in cascade simulations with Pauli blocking for T = 5 MeV initializations (square symbols, disregard star symbols). The black line represents the reference value calculated numerically [17].

from the exact result, while QMD codes with their larger fluctuations deviate considerably more. (The code pBUU uses a stochastic method for the Pauli blocking, which enforces the exact result, while the code CoMD enforces rather strictly $f_i < 1$, which however has other effects which cannot be discussed here, see [17]). In another box calculation, which also cannot be shown here, we investigated inelastic collisions with pion production, which showed non-Markovian effects in the collision sequence of elastic, inelastic and decay processes [18].

Generally it is seen that box calculations allow to study different aspects of simulations in detail and allow to understand the differences between the codes. We especially see how fluctuations sensitively affect many results of calculations, and, in particular, explain the systmatic differences between BUU and QMD codes, due to their different theoretical ansatz to treat fluctuations, as discussed in the theory section.

4 Heavy-ion collisions

Historically, the first TMEP comparisons were performed for HICs, but for the reasons discussed above it was difficult to disentangle and understand the differences between codes [19]. After studying these differences in box calculatons we then returned to HICs and also include pion production via the excitation of the Δ resonance which is of high interest for the determination of the symmetry energy as discussed in the introduction. We compare calculation for a ^{132}Sn+ ^{124}Sn collision at 270 MeV/A [20], as also motivated there. Since HICs are open systems we monitor the evolution of the behaviour of the collision, i.e., the density and asymmetry evolution and the final nucleon observables. We observe also differences here, e.g., of the density evolution, due to effects discussed above in the box-Vlasov comparison. The hope is, that in the charged pion ratios $Y(\pi^-)/Y(\pi^+)$ such differences may partly cancel.

Some results for the pion observables are given in figure 3 as calculated by the different participating codes identified at the bottom. Full symbols represent calculations with Pauli blocking in the usual way and open symbols calculations without it. Some codes (IQMD and TuQMD) apply a correction of the Pauli blocking for the inhomogeneity of phase space at the surface, which is only important in QMD codes. For TuQMD the effect is explicitely shown in the hatched symbol, where this correction is turned off. Panel (a) shows the total pion yields, and demonstrates that Pauli blocking suppresses pion production. We see large differences between the codes, which are mainly due to the different densities reached in the evulution.

Panel (b) shows the corresponding results for the charged pion ratios. The smaller pion yield with Pauli blocking implies a larger ratio, i.e., a larger effect of the symmetry energy. Inspite of forming the pion ratio the differences between the codes are still large, of the order

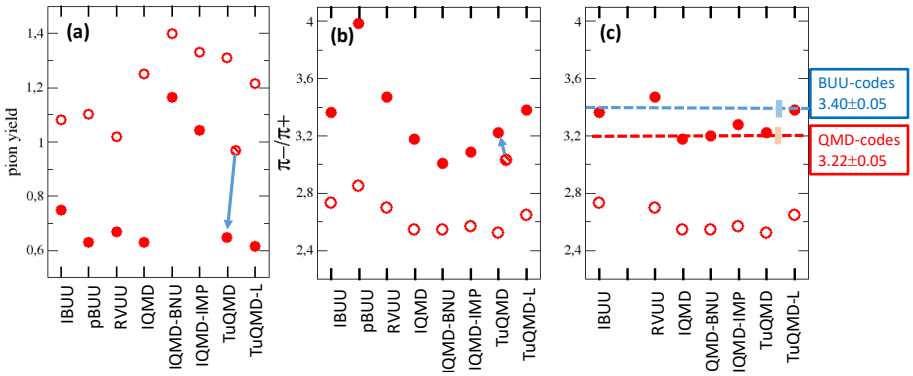

Figure 3. Total pion yield, panel (a), and charged pion ratios, panels (b,c), in ^{132}Sn+^{124}Sn collisions at 270 MeV/A as calculated from various codes identified at the bottom. Full symbols are with Pauli blocking; open symbols without. The hatched symbols in panels (a,b) are TuQMD calculations without a surface correction to Pauli blocking, and the blue arrows show the effect of this. In panel (c) estimated corrections to the results shown in panel (b) are applied, see text.

of 15%. (The results for the code pBUU should be disregarded in this comparison, since here the treatment of the pion and Delta potentials is not exactly the same as in the other codes). However, we can essentially explain these differences, which is sketched in panel (c) (where pBUU is already left out). By comparing calculations of TuQMD with and without Pauli surface corrections (blue arrows) one sees a substantially increased pion ratio. One can then approximately correct the calculations without surface correction (IQMD-BNU and IQMD-IMP) for this effect, which is done in panel (c). Then one observes that the BUU-type codes IBUU, RVUU and TuQMD-L (the last should also be considered BUU-like, see section 2) agree rather well as indicated by the blue dashed horizontal line, within an error of ±0.05 or about ±2%. Also, the QMD-like codes (IQMD,IQMD-BNU, IQMD-IMP, and TuQMD) agree rather well between each other (dashed red line) with about the same error. The difference between the two families is about 0.18, which is seen to agree rather well with the difference between the results of TuQMD and TuQMD-L, which is representative for the systematic difference between BUU- and QMD-type codes due to their different amounts of fluctuations (and here also the evaluation of the non-linar force term). Considering these explainable differences one can state that the codes agree overall to within about ±2%, which is probably within the achievable accuracy of simulations.

5 Discussion and Outlook

The aim of the TMEP code comparisons is to establish quantitatively the robustness of inferences from transport model studies of HICs, which is important to extract information on the EOS and other medium quantities for densities above saturation. For this purpose it is sufficient that the calculations are only semi-realistic, and that important ingredients, like the momentum-dependence of the mean fields, are omitted. Due to extensive studies of box calculations we can largely explain the differences in the different simulations. In particular, we clearly see and understand the systematic differences between the BUU and QMD families of transport descriptions. In some cases we can also recommend optimal strategies, which, however, have not been implemented in all codes at this stage. When approximately taking into acount these understood differences, the codes agree to within approximately 4%.

However, such a code comparison does not say, which simulation codes are most reliable to extract in formation from HICs. In the absence of exact solutions we propose to also consider the comparison to experiment. One should require that a code can realistically describe the global evolution of the phase space, as given by the bulk nucleon observables, like stopping, flow, or nucleon and cluster multiplicities. Only then conclusions from secondary or rare probes, like pions at these energies, can be considered reliable.The uncertainty of transport model analyses as a whole could then be quantified by averaging the distributions of the physics model parameters (e.g., determined by a Bayesian analysis for each code) over the codes weighted by the agreement to bulk observables (and exact results in box calculations). In the multi-messenger era of studies of the equation-of-state of nuclear and stellar matter, an uncertainty quantification of transport model studies is needed.

Acknowledgements

This review is written on behalf of the loosely defined TMEP collaboration, as given, e.g., in the author list of Ref. [5]. The author of this report thanks the organizers of the NRM 2023 for support, and acknowleges support by the Deutsche Forschungsgemeinschaft (DFG, German Research Foundation) under Germany's Excellence Strategy - EXC-2094 - 390783311, ORIGINS.

References

[1] A. Sorensen, et al., Prog. Part. Nucl. Phys. **134** 104080 (2024)
[2] W.G. Lynch, M.B. Tsang, Phys. Lett. B **830** 137098 (2022)
[3] G. Jhang, J. Estee, et al., Phys. Lett. B **813** 136016 (2020)
[4] J. Aichelin, et al., Phys. Rev. Lett. **62**, 1461-1464 (1989)
[5] H. Wolter, et al., Prog. Part. Nucl. Phys. **125** 103962 (2022)
[6] P.C. Martin, J.S. Schwinger, Phys.Rev. **115**, 1342-1373 (1959)
[7] L.P. Kadanoff, G. Baym, *Quantum Statistical Mechanics*, (Benjamin, 1962)
[8] P. Danielewicz, Annals Phys. **152** 239–304 (1984)
[9] W. Botermans, R. Malfliet, Phys. Rep. **198** 115–194 (1990)
[10] P. Danielewicz and G.F. Bertsch, Nucl. Phys. A 533, 712 (1991)
[11] R.J. Lenk, V.R. Pandharipande, Phys. Rev. C **39**, 2242 (1989)
[12] G.F. Bertsch, S. Das Gupta, Phys. Rept. **160** 189–233 (1988)
[13] Y. Abe, S. Ayik, P.G. Reinhard, E. Suraud, Phys. Rep. **275** 49-196 (1996)
[14] J. Aichelin, Phys. Rep. **202**, 233-360 (1991)
[15] A. Ono, Phys. Rev. C **59** 853-864 (1999)
[16] M. Colonna, et al., Phys. Rev. C **104** 024603 (2021)
[17] Y.X. Zhang, Y.J. Wang, et al., Phys. Rev. C **97** 034625 (2018)
[18] Akira Ono, J. Xu, et al., Phys. Rev. C **100** 044617 (2019)
[19] Jun Xu, et al., Phys. Rev. C **93** 044609 (2016)
[20] J. Xu, H. Wolter, et al., Prog. Part. Nucl. Phys., in publication, arcXiv:2308.05347